

Facile Synthesis of Diverse and Functional Nanostructures Derived from a Polyhomocysteine-Based Redox-Responsive Block Copolymer

Molly S. Bickle,[#] Bowen Zhao,[#] Xiao Zhang, Shiwei Fu, and Fuwu Zhang*



Cite This: *ACS Macro Lett.* 2025, 14, 1263–1268



Read Online

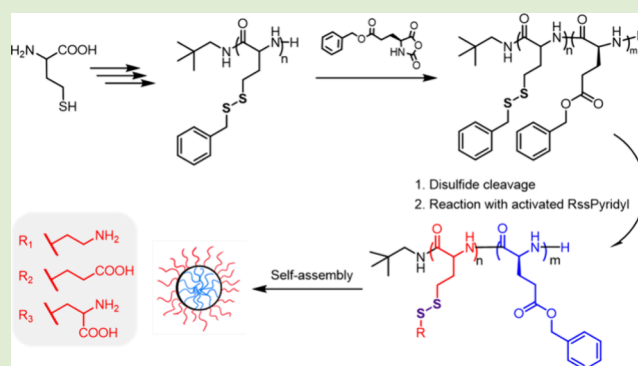
ACCESS |

Metrics & More

Article Recommendations

Supporting Information

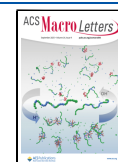
ABSTRACT: Stimuli-responsive polypeptides offer unique advantages for biomedical applications due to their biocompatibility, degradability, and structural tunability. In this study, we report the synthesis of innovative redox-responsive polypeptide-based diblock copolymers consisting of functional disulfide-containing homocysteine derivatives and hydrophobic γ -benzyl-L-glutamate segments via sequential ring-opening polymerizations. The polymerization kinetics revealed that the polymerizations were well-controlled with living characteristics, resulting in diblock copolymers PHcy-*b*-PBLG with narrow molecular weight distributions. The resulting functional-hydrophobic diblock copolymers were further converted to a variety of pendant chains via thiol–disulfide exchange reactions, yielding amphiphilic polymers with tunable surface charges. These disulfide-linked materials readily self-assembled into nanoparticles in aqueous environments with hydrophobic PBLG forming the core and redox-sensitive PHcy forming the shell. The redox-responsive nanoparticles displayed a narrow size distribution, excellent colloidal stability, and excellent biocompatibility. The disulfide bonds within the polymer backbone confer redox sensitivity, allowing potential cleavage in reducing environments. Owing to their tunable surface functionality, redox-responsiveness, and biocompatibility, this platform provides a versatile route to engineer responsive nanostructures for biomedical applications, for example, positively charged nanoparticles toward nucleic acid delivery.

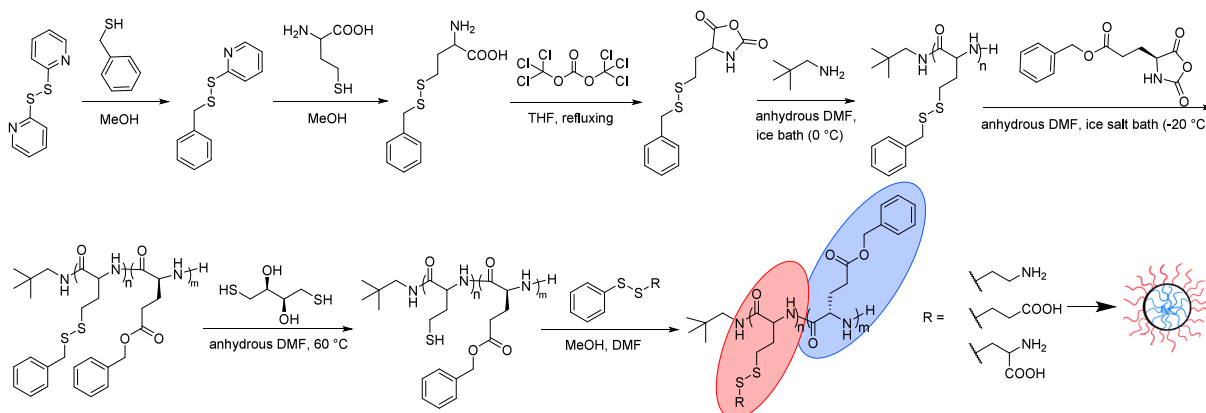


Synthetic polypeptides, derived from naturally occurring amino acids, have attracted significant attention for their potential to serve as functional biomaterials, owing to their biocompatibility, biodegradability, structural versatility, and capacity for self-assembly into diverse nanostructures.^{1–4} Similar to proteins, synthetic polypeptides can form secondary structures, including α -helices and β -sheets, and can be engineered for specific biological interactions while maintaining tunable physicochemical properties.^{5–7} By leveraging the structural diversity of amino acids, these materials exhibit tunable hydrophilicity, redox, pH- and temperature-sensitive behaviors, and functional adaptability for various biomedical applications.^{8–10} In particular, diblock copolypeptides composed of two different types of amino acids are fully degradable and offer unique advantages in material design, enabling precise control over composition, responsiveness to environmental stimuli, and enhanced biocompatibility.^{11–13} For example, amphiphilic block polypeptides can self-assemble into micelles and other types of nanoparticles, with the hydrophobic segments forming the core to encapsulate hydrophobic drugs, while the hydrophilic segments form the shell of the nanoparticle.^{14,15}

Stimuli-responsive materials have attracted extensive attention for their promising potential in biomedical applications.^{16–19} Among them, disulfide-containing polypeptides are highly sought after due to their dynamic covalent disulfide bonds, which are redox-responsive and can be cleaved by free thiols, including glutathione (GSH), a naturally occurring tripeptide that is overexpressed in many diseased tissues within the biological system.^{20–23} For example, polycysteines (PCys) have been widely utilized for a range of biomedical applications, such as tissue engineering, drug delivery, and gene delivery.^{24–26} However, PCys tend to form β -sheet structures, which promote gelation and typically result in short polymer chains with fewer than 20 repeating units.²⁷ Barz and colleagues synthesized activated PCys with low dispersity ($\mathcal{D} < 1.2$) using an S-ethylsulfonyl protecting group. However, the polymer length was still limited due to the formation of β -sheet

Received: April 22, 2025
Revised: August 6, 2025
Accepted: August 7, 2025
Published: August 19, 2025



Scheme 1. Synthesis of Diverse Functional Poly(homocysteine)-Based Diblock Copolymers by Sequential Ring Opening Polymerizations, Followed Post-Polymerization Modification by Thiol–Disulfide Exchange Reactions


structures, leading to gelation and precipitation, thereby restricting the degree of polymerization to less than 30.²⁸ In contrast to PCys, polyhomocysteines derivative (PHD) with a much higher degree of polymerization (>100), which was polymerized from monomers derived from homocysteine, could be readily synthesized due to the absence of β -sheet structure.²⁷ Structurally analogous to cysteine, homocysteine features a similar terminal thiol group, differentiated by an additional carbon atom, which allows for the formation of a redox-responsive disulfide bond. Therefore, PHDs provide exceptional synthetic tunability for designing redox-responsive biocompatible materials suitable for biomedical applications.

In this work, we have developed facile synthesis of redox-responsive polyhomocysteine-based fully degradable diblock copolymers by sequential ring-opening polymerizations (ROPs) of N-carboxyanhydrides (NCAs) of homocysteine and glutamate derivatives (Scheme 1). The polymerizations were investigated in detail, displaying well-controlled first-order polymerization kinetics. Following deprotection, free thiols in the pendant chains could be converted to a range of functional moieties by highly efficient thiol exchange reactions. As a proof of concept, cationic, anionic, and zwitterionic side chains were introduced to the disulfide containing diblock copolymers, resulting in nanoparticles with tunable surface charges and sizes after self-assembly, where hydrophobic poly(γ -benzyl L-glutamate) (PBLG) forms the core of the nanoparticle while disulfide containing PHD serves as the shell.

Polypeptides are commonly synthesized from the NCA of amino acids, a highly reactive five-membered cyclic monomers due to the simplicity and high efficiency of ROPs under mild reaction conditions.^{1,29} In this study, we have designed sequential ROPs to afford fully degradable diblock polypeptides. Neopentylamine was employed as the initiator to polymerize the NCA of homocysteine derivative (Hcy-NCA) and benzyl protected L-glutamate (BLG-NCA) sequentially, resulting in block copolymer PHcy-*b*-PBLG. Benzyl mercaptan was used to protect the thiol group of homocysteine by forming a less reactive disulfide bond. Hcy-NCA was obtained with high yield (>70%) after ring closing by diphosgene. Polymerization reactions were conducted in anhydrous *N,N*-dimethylformamide (DMF) with a constant monomer concentration of 0.5 M for both Hcy-NCA and BLG-NCA. The polymerization reaction of Hcy-NCA proceeded in a

Schlenk flask under a continuous nitrogen flow of 100 mL/min, maintained at 0 °C for 24 h at a monomer-to-initiator molar ratio ($[M]_0/[I]_0$) of 20. Complete polymerization of Hcy-NCA was confirmed by ¹H NMR (Figures S1–S3) and size-exclusion chromatography (SEC). Subsequently, BLG-NCA in DMF (12 equiv to initiator) was added dropwise to the reaction mixture, which was further cooled to –20 °C in an ice-salt bath for better control of polymerization kinetics, better control of the polymerization kinetics, and achieved lower dispersity in the resulting block copolymer. The reaction mixture was stirred at this temperature for an additional 48 h. After complete polymerization of the BLG-NCA as verified by ¹H NMR, the synthesized PHcy-*b*-PBLG block copolymer was purified by precipitating from dichloromethane (DCM) into a mixture of diethyl ether and hexane. This purification process was repeated at least three times to ensure the removal of DMF, potential unreacted monomers, and other impurities.

During the polymerization, aliquots were used to characterize the reaction mixture by using ¹H NMR and FT-IR spectroscopy, and SEC traces were performed to monitor the polymerization progress (Figure 1). In ¹H NMR spectra, the *tert*-butyl group of the initiator neopentylamine exhibited a distinct singlet at 0.8 ppm labeled as peak *a* in Figure 1a, which served as a reference peak for end group analysis. The methine proton in the polyhomocysteine backbone, along with benzylic protons and benzyl aromatic protons in the side chains, labeled as peaks *e*, *f*, and *g*, respectively, could be used to calculate the degree of polymerization (DP) of PHcy. A DP of 20 was determined accordingly, suggesting the complete conversion of the Hcy-NCA monomer to the polymer. SEC demonstrated that monomodal distribution of molar mass of PHcy, with a dispersity (\mathcal{D}) value of 1.15 (Figure 1b, blue trace). In the ¹H NMR spectra, a new peak at 5.1 ppm, corresponding to the benzylic protons from the polyglutamate (PBLG), emerged, indicating the successful chain extension with BLG-NCA monomers to afford diblock copolymer PHcy-*b*-PBLG. The integration value of 24 suggested a nearly complete addition of the BLG-NCA monomer to the polymer. Furthermore, the peaks labeled “*h* and *i*” at 4.4 ppm, corresponding to the protons attached to the methine carbons in the polymer backbone of both PHcy and PBLG blocks, respectively, appeared broader after the block polymer formation compared to those in PHcy. The integration value of the “*h* and *i*” peak

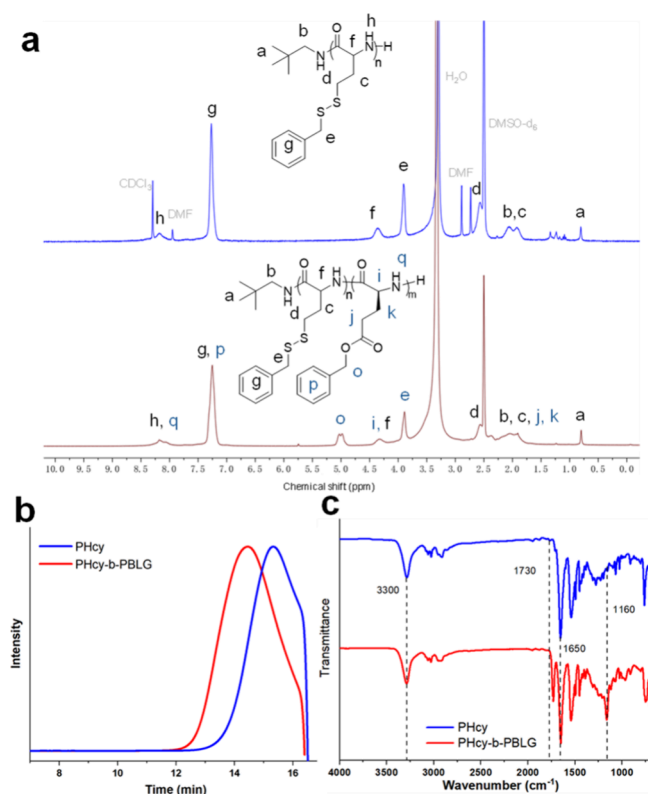


Figure 1. (a) ^1H NMR spectra of PHcy-*b*-PBLG and PHcy, where n is 20 and m is 12. (b) SEC traces and (c) FT-IR spectra of PHcy (blue) and PHcy-*b*-PBLG (red).

was calculated to be 32, aligning with the expected proton integration based on the polymer's stoichiometry of 20 repeating units of homocysteine and 12 repeating units of glutamate. Additionally, the decrease in retention time of PHcy-*b*-PBLG compared with PHcy in the SEC indicated a higher molar mass, further demonstrating the successful chain extension from homopolymer PHcy (Figure 1b). The IR spectrum of the block polymer displayed several peaks that corresponded to functional groups in the final polymer structure.³⁰ The sharp peak seen at 3300 cm^{-1} represented the amide N–H in the backbone of the polymer, while in the sharp peak at 1650 cm^{-1} indicated the backbone's amide C=O bonds. The peaks at 1730 and 1160 cm^{-1} demonstrated the presence of ester bonds from polyglutamate PBLG.

Maintaining a low reaction temperature is critical for achieving controlled ROP of NCA monomers.²⁹ Deming et al. demonstrated that polymerizations conducted at $0\text{ }^\circ\text{C}$ retained living amine chain-ends in 99% of the chains, which was essential for the successful synthesis of block copolymers.²⁹ Lower temperatures slow down both the initiation and propagation steps, enabling better control over polymerization kinetics and resulting in a narrower molecular weight distribution.²⁷ Given the high reactivity of NCA monomers, moderately low temperatures are particularly advantageous, as they improve monomer conversion while minimizing side reactions. In this work, the ROP of Hcy-NCA was carried out at $0\text{ }^\circ\text{C}$ (using an ice bath) to preserve the living character of the chain ends. However, when BLG-NCA was polymerized using PHcy-NH₂ as the macroinitiator, an even lower temperature ($-20\text{ }^\circ\text{C}$, achieved with an ice-salt bath) was required. This difference in optimal temperatures likely arises

from the higher reactivity of BLG-NCA, necessitating stricter thermal control to prevent unwanted side reactions and ensure well-defined block copolymer formation. Worth noting, switching the polymerization sequence by polymerizing BLG-NCA first led to a multimodal distribution of molar mass with large dispersities.

The polymerization kinetics of the ROP of Hcy-NCA and BLG-NCA were investigated using the same $[M]_0/[I]_0$ ratio as previously discussed, in anhydrous DMF with the same initiator (Figure 2). The SEC traces (Figure 2a) showed

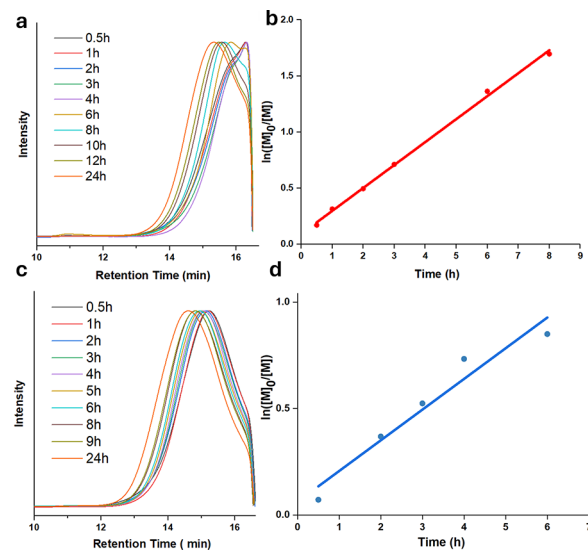


Figure 2. Kinetics study of PHcy block and poly(glutamate) block. (a) GPC traces of neopentylamine-poly(homocysteine) over the first 24 h of polymerization. (b) Monomer conversion $\ln([M]_0/[M])$ vs time calculated from the ^1H NMR spectra taken during polymerization of PHcy block. (c) GPC elution of PHcy-*b*-PBLG over the first 24 h of polymerization of PBLG block. (d) Monomer conversion $\ln([M]_0/[M])$ vs time calculated from the ^1H NMR spectra taken during polymerization of PBLG block.

monomodal peaks that gradually shifted toward shorter elution times as the polymerization proceeded, indicating increasing molecular weight and relatively narrow dispersities ($D \leq 1.15$) during polymerization of the PHcy block. Linear plots of $\ln([M]_0/[M])$ versus time (Figure 2b) demonstrated first-order kinetics. The living nature of the polymerization was further evidenced by the successful chain extension with BLG-NCA monomers. In this step, the SEC traces (Figure 2c) continued to display monomodal peaks shifting toward shorter elution times, with dispersities remaining relatively low ($D \leq 1.25$). The corresponding kinetic plots (Figure 2d) also showed linearity, confirming first-order kinetics and supporting a controlled block copolymerization process.^{23,31}

Postpolymerization modifications offer a straightforward and effective strategy for introducing diverse functional groups into polymer side chains.^{1,32} In contrast, directly polymerizing functional monomers often leads to inefficiencies and poorly controlled reactions due to incompatibilities between the functional groups and the polymerization conditions.^{33,34} In this study, we successfully conjugated various pendant functional groups (R groups), including positively charged cysteamine hydrochloride, 3-mercaptopropionic acid, and zwitterionic cysteine, onto the PHcy-*b*-PBLG backbone via facile thiol–disulfide exchange reactions (Figure 3a). Thiol–

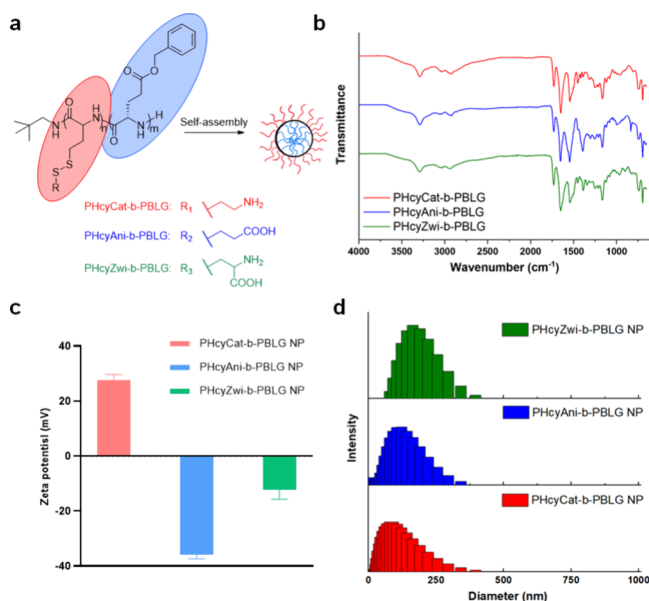


Figure 3. Comparison of PHcyCat-*b*-PBLG, PHcyAni-*b*-PBLG, and PHcyZwi-*b*-PBLG. (a) The complete block polymer with the various side chains formed a nanoparticle through self-assembly in water. (b) FT-IR spectra of each polymer before self-assembly. (c) Zeta potential measurement and (d) DLS analysis of nanoparticles formed from PHcyCat-*b*-PBLG, PHcyAni-*b*-PBLG, and PHcyZwi-*b*-PBLG.

disulfide exchange reactions could be performed under mild conditions, enabling the responsiveness.³⁵ The disulfide bonds were first deprotected by excess dithiothreitol (DTT) to expose free thiol groups in the side chains in PHcy-*b*-PBLG. DMF was selected as the optimal solvent due to its excellent ability to dissolve the polymer. Complete deprotection of the benzyl mercaptan groups was achieved by using with excess DTT in anhydrous DMF at 60 °C for 48 h. The product was purified by precipitating DCM into a mixture of diethyl ether and hexane. ¹H NMR analysis confirmed nearly quantitative deprotection, as evidenced by the disappearance of methylene peaks ($\delta = 3.8$, labeled as e in Figure 1a) and significant reduction of the integration of aromatic proton ($\delta = 7.5$ – 7.0 ppm, Figure S6). At the same time, thiol containing functional moieties were activated with dithiodipyridine to form reactive pyridyl disulfide (RssPy). Subsequently, deprotected polymers were then functionalized by treating them with excess of RssPy (5 equiv relative to thiol groups) in anhydrous DMF for 48 h. The resulting modified polymers, designated as PHcyR-*b*-PBLG (R = Cat, Ani, or Zwi), were purified by dialysis against water for 2 days. Successful functionalization was indicated by FT-IR (Figure 3b) as evidenced by differences in the fingerprint region (below 1500 cm⁻¹) and was further confirmed by ¹H NMR (Figures S7–S9).³⁶ High substitutions of the pendant groups were achieved according to ¹H NMR spectra (Figures S7–S9). After functionalization, the disulfide-containing polymers could be readily redissolved in DMSO after storage in a refrigerator for several months, whereas the deprotected polymer became insoluble within 1 week even when stored in a nitrogen-filled vial. The ease and flexibility of modifying pendant chains highlight the strengths of our approach, where a series of redox-responsive polypeptides could be obtained from the same parent diblock polypeptides toward different biomedical applications. Multiple responsive functionalities could be potentially installed at the same time,

offering precise control over polymer properties and promising broad applicability in biomedical fields.^{11,37}

The obtained amphiphilic diblock polypeptides were then self-assembled into nanoparticles (NPs) with diverse properties, demonstrating their potential for various biomedical applications.²³ Stock solutions of three different polymers were prepared in DMSO at a concentration of 5 mg/mL, respectively. Then aliquots of stock solution were added dropwise into water under stirring, reaching a final concentration of 50 μ g/mL. The hydrophobic PBLG segments formed the core of the NPs, while the hydrophilic pendant groups from PHcy constituted the outer shell in the aqueous media. Surface zeta potential measurements confirmed the designed surface charges of the NPs (Figure 3c). Specifically, Amino groups containing PHcyCat-*b*-PBLG NPs exhibited a positive zeta potential of $+28 \pm 2$ mV, demonstrating their potential as carriers for nucleic acids via electrostatic interactions. Carboxylic acid containing PHcyAni-*b*-PBLG NPs exhibited a negative zeta potential of -36 ± 1 mV, while zwitterionic PHcyZwi-*b*-PBLG NPs showed a reduced negative surface charge of -12 ± 4 mV. Dynamic light scattering (DLS) analysis revealed that the hydrodynamic diameters of the positively charged PHcyCat-*b*-PBLG NPs, negatively charged PHcyAni-*b*-PBLG NPs, and zwitterionic PHcyZwi-*b*-PBLG NPs were approximately 100, 150, and 200 nm, respectively, all with similar polydispersity indices (Figure 3d and Table S1). Circular transmission electron microscopy (TEM) images showed that the diameters of these NPs were approximately 30–40 nm (Figure S10). No signs of aggregation or precipitation were observed after several months of storage at 4 °C in the refrigerator, indicating the excellent colloidal and hydrolytic stability of the nanoparticles (Table S2). The *in vitro* cytotoxicity of the synthesized polymers was evaluated by using the 4T1 cell line (Figure 4).

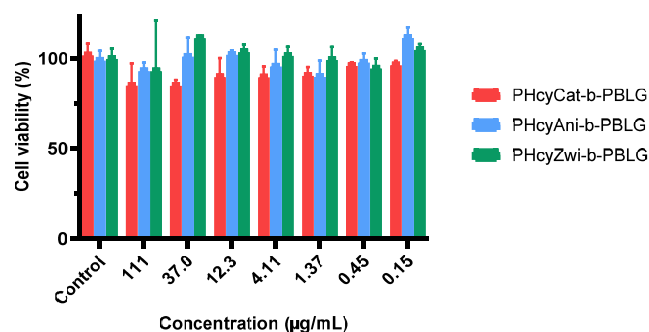


Figure 4. *In vitro* cytotoxicity of PHcyR-*b*-PBLG NPs against 4T1 cells after 24 h incubation at 37 °C and 5% CO₂.

PHcyCat-*b*-PBLG nanoparticles, which carry a positively charged surface, maintained over 70% cell viability at concentrations up to 110 μ g/mL, indicating excellent biocompatibility. This is in contrast to many positively charged polymers, for example, polyethylene imine had less than 50% cell viability at ~ 10 μ g/mL. Furthermore, PHcyAni-*b*-PBLG and PHcyZwi-*b*-PBLG, both exhibiting negative zeta potentials, showed negligible cytotoxicities, demonstrating excellent compatibility with 4T1 cells. Calcein-AM/PI double staining of 4T1 cancer cells treated with PHcyR-*b*-PBLG (R = Cat, Ani, and Zwi) for 24 h indicated minimal disruption to cell membrane integrity, with the majority of cells remaining viable, consistent with the *in vitro* cytotoxicity results. (Figure S11)

This enhanced biocompatibility is likely due to the absence of surface positive charge, which reduces interactions with the negatively charged cell membrane and thereby minimizes membrane disruption and cellular stress.

In summary, a new class of stimuli-responsive diblock polypeptides was developed by sequential ROPs of functional disulfide-containing homocysteine-derived monomers and hydrophobic glutamate monomers. The polymerization kinetics revealed that the polymerizations were well-controlled with living characteristics, resulting diblock copolymers PHcy-*b*-PBLG with narrow molecular weight distributions. Post-polymerization modification via thiol–disulfide exchange enabled the introduction of diverse functional groups, yielding amphiphilic polymers with tunable surface charges. These disulfide-linked materials readily self-assembled into nanoparticles in aqueous media with hydrophobic PBLG forming the core and redox-sensitive PHcy forming the shell. The disulfide bonds in the shell confer redox responsiveness, allowing for triggered cleavage under reductive conditions. The redox-responsive nanoparticles displayed narrow size distribution, excellent colloidal stability, and excellent biocompatibility. Ongoing efforts aim to explore these materials as building blocks for a wide range of biomedical applications, especially positively charged nanoparticles for nucleic acid delivery.

■ ASSOCIATED CONTENT

SI Supporting Information

The Supporting Information is available free of charge at <https://pubs.acs.org/doi/10.1021/acsmacrolett.5c00270>.

Materials, methods, and experimental details; Polymer characterization (PDF)

■ AUTHOR INFORMATION

Corresponding Author

Fuwu Zhang – Department of Chemistry, University of Miami, Coral Gables, Florida 33146, United States; The Dr. John T. Macdonald Foundation Biomedical Nanotechnology Institute, University of Miami, Miami, Florida 33136, United States; Sylvester Comprehensive Cancer Center, University of Miami Miller School of Medicine, Miami, Florida 33136, United States; orcid.org/0000-0002-1928-3472;
Email: fxz174@miami.edu

Authors

Molly S. Bickle – Department of Chemistry, University of Miami, Coral Gables, Florida 33146, United States
Bowen Zhao – Department of Chemistry, University of Miami, Coral Gables, Florida 33146, United States
Xiao Zhang – Department of Chemistry, University of Miami, Coral Gables, Florida 33146, United States
Shiwei Fu – Department of Chemistry, University of Miami, Coral Gables, Florida 33146, United States; orcid.org/0009-0004-3702-2163

Complete contact information is available at: <https://pubs.acs.org/doi/10.1021/acsmacrolett.5c00270>

Author Contributions

[#]M.S.B. and B.Z. contribute equally to this work. The manuscript was written through contributions of all authors. M.S.B. and B.Z.: Conceptualization, Methodology, Validation, Formal analysis, Data curation, Investigation, Writing-original draft, Writing-review and editing, Project administration. X.Z.:

Formal analysis, Data curation. S.F.: Formal analysis, Data curation. F.Z.: Conceptualization, Funding acquisition, Resources, Supervision, Visualization, Methodology, Project administration, Writing-review and editing.

Notes

The authors declare no competing financial interest.

■ ACKNOWLEDGMENTS

This work is supported by the National Science Foundation CAREER award under Grant No. 2238812.

■ REFERENCES

- (1) Deming, T. J. Synthesis of Side-Chain Modified Polypeptides. *Chem. Rev.* **2016**, *116* (3), 786–808.
- (2) He, C.; Zhuang, X.; Tang, Z.; Tian, H.; Chen, X. Stimuli-sensitive synthetic polypeptide-based materials for drug and gene delivery. *Adv. Healthc. Mater.* **2012**, *1* (1), 48–78.
- (3) Yorke, S. K.; Yang, Z.; Wiita, E. G.; Kamada, A.; Knowles, T. P. J.; Buehler, M. J. Design and sustainability of polypeptide material systems. *Nature Reviews Materials* **2025**, DOI: [10.1038/s41578-025-00793-3](https://doi.org/10.1038/s41578-025-00793-3).
- (4) Chen, G.; Zhao, B.; Ruiz, E. F.; Zhang, F. Advances in the polymeric delivery of nucleic acid vaccines. *Theranostics* **2022**, *12* (9), 4081–4109.
- (5) Kumar, R.; Santa Chalarca, C. F.; Bockman, M. R.; Bruggen, C. V.; Grimme, C. J.; Dalal, R. J.; Hanson, M. G.; Hexum, J. K.; Reineke, T. M. Polymeric Delivery of Therapeutic Nucleic Acids. *Chem. Rev.* **2021**, *121* (18), 11527–11652.
- (6) Yang, Z.; Lin, L.; Guo, Z.; Guo, X.; Tang, Z.; Tian, H.; Chen, X. Synthetic Helical Polypeptide as a Gene Transfection Enhancer. *Biomacromolecules* **2022**, *23* (7), 2867–2877.
- (7) Coulter, S. M.; Pentlavalli, S.; An, Y.; Vora, L. K.; Cross, E. R.; Moore, J. V.; Sun, H.; Schweins, R.; McCarthy, H. O.; Laverty, G. In Situ Forming, Enzyme-Responsive Peptoid-Peptide Hydrogels: An Advanced Long-Acting Injectable Drug Delivery System. *J. Am. Chem. Soc.* **2024**, *146* (31), 21401–21416.
- (8) Li, Y.; Yang, G.; Gerstweiler, L.; Thang, S. H.; Zhao, C.-X. Design of Stimuli-Responsive Peptides and Proteins. *Adv. Funct. Mater.* **2023**, *33*, 2210387.
- (9) He, X.; Fan, J.; Wooley, K. L. Stimuli-Triggered Sol-Gel Transitions of Polypeptides Derived from alpha-Amino Acid N-Carboxyanhydride (NCA) Polymerizations. *Chem. Asian J.* **2016**, *11* (4), 437–47.
- (10) Shi, Y.; Li, D.; Ding, J.; He, C.; Chen, X. Physiologically relevant pH- and temperature-responsive polypeptide hydrogels with adhesive properties. *Polym. Chem.* **2021**, *12* (19), 2832–2839.
- (11) Morrison, C. A.; Chan, E. P.; Deming, T. J. Triggered Inversion of Dual Responsive Diblock Copolymer Vesicles. *J. Am. Chem. Soc.* **2025**, *147* (9), 7617–7623.
- (12) Fan, J.; Li, R.; Wang, H.; He, X.; Nguyen, T. P.; Letteri, R. A.; Zou, J.; Wooley, K. L. Multi-responsive polypeptide hydrogels derived from N-carboxyanhydride terpolymerizations for delivery of non-steroidal anti-inflammatory drugs. *Org. Biomol. Chem.* **2017**, *15* (24), 5145–5154.
- (13) Klemm, P.; Solomun, J. I.; Rodewald, M.; Kuchenbrod, M. T.; Hansch, V. G.; Richter, F.; Popp, J.; Hertweck, C.; Hoepfner, S.; Bonduelle, C.; Lecommandoux, S.; Traeger, A.; Schubert, S. Efficient Gene Delivery of Tailored Amphiphilic Polypeptides by Polyplex Surfing. *Biomacromolecules* **2022**, *23* (11), 4718–4733.
- (14) Zhao, B.; Zhang, X.; Bickle, M. S.; Fu, S.; Li, Q.; Zhang, F. Development of polypeptide-based materials toward messenger RNA delivery. *Nanoscale* **2024**, *16* (5), 2250–2264.
- (15) Ahmadi, V.; Zabihi, F.; Rancan, F.; Staszak, A. A.; Nie, C.; Dimde, M.; Achazi, K.; Wiehe, A.; Vogt, A.; Haag, R. Amphiphilic Copolypeptides Self-Assembled into Spherical Nanoparticles for Dermal Drug Delivery. *ACS Applied Nano Materials* **2021**, *4* (7), 6709–6721.

- (16) Pallavi, P.; Girigoswami, K.; Harini, K.; Gowtham, P.; Thirumalai, A.; Girigoswami, A. Theranostic dye entrapped in an optimized blended-polymer matrix for effective photodynamic inactivation of diseased cells. *Naunyn Schmiedebergs Arch Pharmacol* **2025**, *398* (1), 867–880.
- (17) Thirumalai, A.; Girigoswami, K.; Harini, K.; Kiran, V.; Durgadevi, P.; Girigoswami, A. Natural polymer derivative-based pH-responsive nanoformulations with entrapped diketo-tautomers of 5-fluorouracil for enhanced cancer therapy. *ADMET & DMPK* **2024**, *13* (1), 2554.
- (18) Miglani, C.; Ralhan, J.; Banoo, M.; Nath, D.; Sil, S.; Pal, S. K.; Gautam, U. K.; Pal, A. Stimuli-Responsive Control over Self-Assembled Nanostructures in Sequence-Specific Functional Block Copolymers. *ACS Polym. Au* **2024**, *4* (3), 255–265.
- (19) Miglani, C.; Banoo, M.; Nath, D.; Ralhan, J.; Sil, S.; Joseph, J. P.; Pal, S. K.; Gautam, U.; Pal, A. Orthogonal chain collapse in stimuli-responsive di-block polymers leading to self-sorted nanostructures. *Chem. Commun. (Camb)* **2023**, *59* (88), 13195–13198.
- (20) Lee, M. H.; Yang, Z.; Lim, C. W.; Lee, Y. H.; Dongbang, S.; Kang, C.; Kim, J. S. Disulfide-cleavage-triggered chemosensors and their biological applications. *Chem. Rev.* **2013**, *113* (7), 5071–109.
- (21) Zhang, X.; Zhao, B.; Fu, S.; Seruya, R. S.; Fanos, H. E.; Petrisor, A. A.; Liu, Y.; Yang, Z.; Zhang, F. Controlling stimulus sensitivity by tailoring nanoparticle core hydrophobicity. *Biomater Sci.* **2025**, *13*, 2332–2339.
- (22) Zhang, F.; Ni, Q.; Jacobson, O.; Cheng, S.; Liao, A.; Wang, Z.; He, Z.; Yu, G.; Song, J.; Ma, Y.; Niu, G.; Zhang, L.; Zhu, G.; Chen, X. Polymeric Nanoparticles with a Glutathione-Sensitive Heterodimeric Multifunctional Prodrug for In Vivo Drug Monitoring and Synergistic Cancer Therapy. *Angew. Chem., Int. Ed. Engl.* **2018**, *57* (24), 7066–7070.
- (23) Zhang, X.; Zhao, B.; Fu, S.; Seruya, R. S.; Madey, J. F.; Bukhryakova, E.; Zhang, F. Rapid and Versatile Synthesis of Glutathione-Responsive Polycarbonates from Activated Cyclic Carbonates. *Macromolecules* **2024**, *57* (6), 2858–2867.
- (24) Zhang, J. L.; Li, K.; Zhang, Q. R.; Zhu, Z. M.; Huang, G. C.; Tian, H. Q. Polycysteine as a new type of radio-protector ameliorated tissue injury through inhibiting ferroptosis in mice. *Cell Death Dis* **2021**, *12* (2), 1–16.
- (25) Wu, T.; Wang, L.; Ding, S.; You, Y. Fluorinated PEG-Polypeptide Polyplex Micelles Have Good Serum-Resistance and Low Cytotoxicity for Gene Delivery. *Macromol. Biosci.* **2017**, *17* (8), 1700114.
- (26) Kareem, Y. G.; Rachid, S.; Al-Jaf, O. Synthesis and characterization of novel poly cysteine methacrylate nanoparticles and their morphology and size studies. *RSC Adv.* **2024**, *14* (19), 13474–13481.
- (27) Muhl, C.; Schäfer, O.; Bauer, T.; Räder, H.; Barz, M. Poly(S-ethylsulfanyl-l-homocysteine): An α -Helical Polypeptide for Chemo-selective Disulfide Formation. *Macromolecules* **2018**, *51* (20), 8188–8196.
- (28) Schäfer, O.; Huesmann, D.; Barz, M. Poly(S-ethylsulfanyl-l-cysteines) for Chemoselective Disulfide Formation. *Macromolecules* **2016**, *49* (21), 8146–8153.
- (29) Cheng, J.; Deming, T. J. Synthesis of polypeptides by ring-opening polymerization of alpha-amino acid N-carboxyanhydrides. *Top. Curr. Chem.* **2011**, *310*, 1–26.
- (30) Lu, H.; Wang, J.; Bai, Y.; Lang, J. W.; Liu, S.; Lin, Y.; Cheng, J. Ionic polypeptides with unusual helical stability. *Nat. Commun.* **2011**, *2*, 206.
- (31) Wang, H.; Su, L.; Li, R.; Zhang, S.; Fan, J.; Zhang, F.; Nguyen, T. P.; Wooley, K. L. Polyphosphoramidates That Undergo Acid-Triggered Backbone Degradation. *ACS Macro Lett.* **2017**, *6* (3), 219–223.
- (32) Lin, Y.-N.; Khan, S.; Song, Y.; Dong, M.; Shen, Y.; Tran, D. K.; Pang, C.; Zhang, F.; Wooley, K. L. A Tale of Drug-Carrier Optimization: Controlling Stimuli Sensitivity via Nanoparticle Hydrophobicity through Drug Loading. *Nano Lett.* **2020**, *20* (9), 6563–6571.
- (33) Zhang, X.; Zhao, B.; Fu, S.; Liu, Y.; Petrisor, A. A.; Yang, Z.; Fanos, H. E.; Seruya, R. S.; Zhang, F. Redox-Responsive Cross-Linking of Polycarbonate Nanomedicines for Enhanced Stability and Controlled Drug Delivery. *ACS Appl. Mater. Interfaces* **2025**, *17* (15), 23135–23145.
- (34) Liu, Y.; Yin, L. α -Amino acid N-carboxyanhydride (NCA)-derived synthetic polypeptides for nucleic acids delivery. *Adv. Drug Delivery Rev.* **2021**, *171*, 139–163.
- (35) Yoon, J. A.; Kamada, J.; Koynov, K.; Mohin, J.; Nicolay, R.; Zhang, Y.; Balazs, A. C.; Kowalewski, T.; Matyjaszewski, K. Self-Healing Polymer Films Based on Thiol–Disulfide Exchange Reactions and Self-Healing Kinetics Measured Using Atomic Force Microscopy. *Macromolecules* **2012**, *45* (1), 142–149.
- (36) Fan, J.; Li, R.; He, X.; Seetho, K.; Zhang, F.; Zou, J.; Wooley, K. L. Construction of a versatile and functional nanoparticle platform derived from a helical diblock copolypeptide-based biomimetic polymer. *Polym. Chem-Uk* **2014**, *5* (13), 3977–3981.
- (37) Fu, S.; Rempson, C. M.; Puche, V.; Zhao, B.; Zhang, F. Construction of disulfide containing redox-responsive polymeric nanomedicine. *Methods* **2022**, *199*, 67–79.